AIP | Advances

Investigating the electronic properties of Al2O3/Cu(In,Ga)Se2 interface

R. Kotipalli, B. Vermang, J. Joel, R. Rajkumar, M. Edoff, and D. Flandre

Citation: AIP Advances **5**, 107101 (2015); doi: 10.1063/1.4932512
View online: http://dx.doi.org/10.1063/1.4932512
View Table of Contents: http://scitation.aip.org/content/aip/journal/adva/5/10?ver=pdfcov
Published by the AIP Publishing

Investigating the electronic properties of Al_2O_3/Cu(In, Ga)Se_2 interface

R. Kotipalli,[1,a,b] B. Vermang,[2,3,4,a,c] J. Joel,[2] R. Rajkumar,[1] M. Edoff,[2] and D. Flandre[1]
[1]*ICTEAM, Université catholique de Louvain, Louvain-la-Neuve, 1348, Belgium*
[2]*Ångström Solar Center, University of Uppsala, Uppsala, 75121, Sweden*
[3]*ESAT-KU Leuven, University of Leuven, Leuven, 3001, Belgium*
[4]*IMEC, Kapeldreef 75, Leuven, 3001, Belgium*

(Received 7 July 2015; accepted 17 September 2015; published online 1 October 2015)

Atomic layer deposited (ALD) Al_2O_3 films on Cu(In,Ga)Se_2 (CIGS) surfaces have been demonstrated to exhibit excellent surface passivation properties, which is advantageous in reducing recombination losses at the rear metal contact of CIGS thin-film solar cells. Here, we report, for the first time, experimentally extracted electronic parameters, i.e. fixed charge density (Q_f) and interface-trap charge density (D_{it}), for as-deposited (AD) and post-deposition annealed (PDA) ALD Al_2O_3 films on CIGS surfaces using capacitance–voltage (C-V) and conductance-frequency (G-f) measurements. These results indicate that the AD films exhibit positive fixed charges Q_f (approximately 10^{12} cm^{-2}), whereas the PDA films exhibit a very high density of negative fixed charges Q_f (approximately 10^{13} cm^{-2}). The extracted D_{it} values, which reflect the extent of chemical passivation, were found to be in a similar range of order (approximately 10^{12} cm^{-2} eV^{-1}) for both AD and PDA samples. The high density of negative Q_f in the bulk of the PDA Al_2O_3 film exerts a strong Coulomb repulsive force on the underlying CIGS minority carriers (n_s), preventing them to recombine at the CIGS/Al_2O_3 interface. Using experimentally extracted Q_f and D_{it} values, SCAPS simulation results showed that the surface concentration of minority carriers (n_s) in the PDA films was approximately eight-orders of magnitude lower than in the AD films. The electrical characterization and estimations presented in this letter construct a comprehensive picture of the interfacial physics involved at the Al_2O_3/CIGS interface. [http://dx.doi.org/10.1063/1.4932512]

Most recently, a new world record conversion efficiency of 21.7% has been reported for thin-film solar cells based on CIGS.[1] Current approaches and future priorities within the CIGS photovoltaic community are focused on passivation concepts to reduce carrier recombination at interfaces and to enhance cell efficiencies. These approaches involve novel methods to passivate the front and rear surface of the CIGS absorber by (i) implementing alkali post-deposition treatments at the front surface,[1–3] (ii) passivating the rear surface of the CIGS/Mo interface using ALD Al_2O_3 films,[4,5] and (iii) implementing back surface field-effect passivation using gallium grading schemes within the CIGS absorber layer.[6]

In our previous studies,[4,5] we reported that Al_2O_3 rear-surface passivation of ultra-thin CIGS solar cells can significantly enhance the open-circuit voltage (V_{oc}) due to a reduced rear surface recombination velocity at the CIGS/Mo interface, ultimately leading to a notable enhancement in cell efficiency [i.e., by more than 3.5% (abs.)] compared with corresponding unpassivated reference

[a]R. Kotipalli and B. Vermang contributed equally to this work.
[b]Electronic mail: raja.kotipalli@uclouvain.be
[c]Electronic mail: bart.vermang@imec.be

cells. Additionally, the rear surface recombination rate has been qualitatively addressed in Ref. 7 by means of photoluminescence (PL) measurements, where an elevated PL intensity by one order of magnitude was seen for passivated CIGS absorbers compared with unpassivated. Such improvements in the cell efficiencies and PL intensity led us to characterize the electronic properties of the Al_2O_3/CIGS interface and the dominant passivation mechanism involved. W.W. Hsu et al.[8] reported that introducing ALD Al_2O_3 passivation films on CIGS surfaces could reduce the effective surface recombination velocity (S_{eff}) to 14–44 cm/s. Such low S_{eff} values for Al_2O_3 passivated CIGS surfaces are attributed to an adequate field-effect passivation in combination with an improved chemical passivation.

The concept of passivating CIGS surfaces using ALD Al_2O_3 films is based on previous experience gained from silicon solar cell technologies.[9–12] The surface passivation of silicon substrates using ALD Al_2O_3 films has drawn intense attention from the silicon photovoltaic community because of these films' ability to passivate p- and n-type as well as highly doped p^+ silicon surfaces effectively.[9,10] This passivation ability is attributed to a high density of negative Q_f (10^{12}–10^{13} cm^{-2}) in the Al_2O_3 bulk (field-effect passivation) in combination with a low interface-trap charge density D_{it} (10^{10}–10^{12} eV^{-1} cm^{-2}) at the Al_2O_3/Silicon interface (chemical passivation).[9–12] Therefore, in the case of CIGS surface passivation by ALD Al_2O_3, experimentally extracting these electronic properties is important (i) to evaluate the passivation quality, and (ii) to understand the dominant passivation mechanism involved.

In this study, are for the first time experimentally extracted Q_f and D_{it} values for ALD Al_2O_3-passivated CIGS surfaces reported. These values were extracted by characterizing capacitance vs. voltage and frequency (C–V–ω) and conductance vs. frequency and temperature (G–ω–T) at different voltages on metal–insulator–semiconductor (MIS) structures. The MIS structures consists of a 350 nm thick molybdenum back contact sputtered on a soda-lime glass (SLG) substrate, followed by a 2 μm thick CIGS absorber layer (with uniform gallium profile) co-evaporated at 510°C. A 22.5 nm thick Al_2O_3 film was deposited on the CIGS surfaces in a temporal ALD reactor at 300°C using trimethylaluminum and water as precursors. The thickness of the Al_2O_3 film was monitored by the growth rate (0.9 Å/cycle). Finally, aluminum front contacts, with a contact area of 7.8×10^{-3} cm^2, were evaporated through a shadow mask. The influence of annealing treatment on the passivation quality was examined by fabricating two sets of MIS structures: (i) AD Al_2O_3 films (i.e., non-annealed) on CIGS surfaces and (ii) post-deposition annealed Al_2O_3 films (at 510°C in a selenium (Se) atmosphere) on CIGS surfaces. At this point it is important to note that the post-deposition annealing treatment performed in our experiments is not a "special anneal" but "a way to mimic the processing of rear passivated CIGS solar cells", where the CIGS layer is grown (at the same temperature and in the same Se atmosphere as the anneal used) on top of the passivation layer. On the other hand, it also enables us to investigate the effects of annealing treatment on the electronic properties of Al_2O_3/CIGS interface.[3,4]

To quantify and evaluate the electronic properties of the AD and PDA films, a detailed electrical characterization was performed using C–V–G measurements on MIS structures in order to extract the Q_f and D_{it} values. Fig. 1(a) depicts the C–V characteristics of the AD and PDA films measured at 10 kHz. In the case of the AD films, a depletion/weak-inversion transition region occurring at negative applied gate voltages was observed, whereas the transition region occurred at positive gate voltages for the PDA films. The corresponding flatband voltage (V_{fb}) positions are attributed to the polarity and concentration of Q_f present in the films.[11–14]

Fig. 1(b) and 1(c) shows the C–V curves at different frequencies for AD and PDA films. As can be seen in Fig. 1(b) and 1(c), the C-V curves show strong frequency dispersion effects in the accumulation regime. One possible explanation from the literature that can be put forward to explain the observed parasitic effects is due to the "oxide, near interface traps and border traps," residing in the oxide.[15–18] These traps communicate with the underlying semiconductor electrons/holes by tunneling mechanism and the associated time constant depends on the trap distance to the interface, giving rise to frequency dispersion.[15,19] These parasitic effects will alter the measured capacitance-conductance (C-G) values, which will in turn affect the interpreted D_{it} up to an order of magnitude. Therefore, to minimize the influence of these effects on the extracted interface electronic

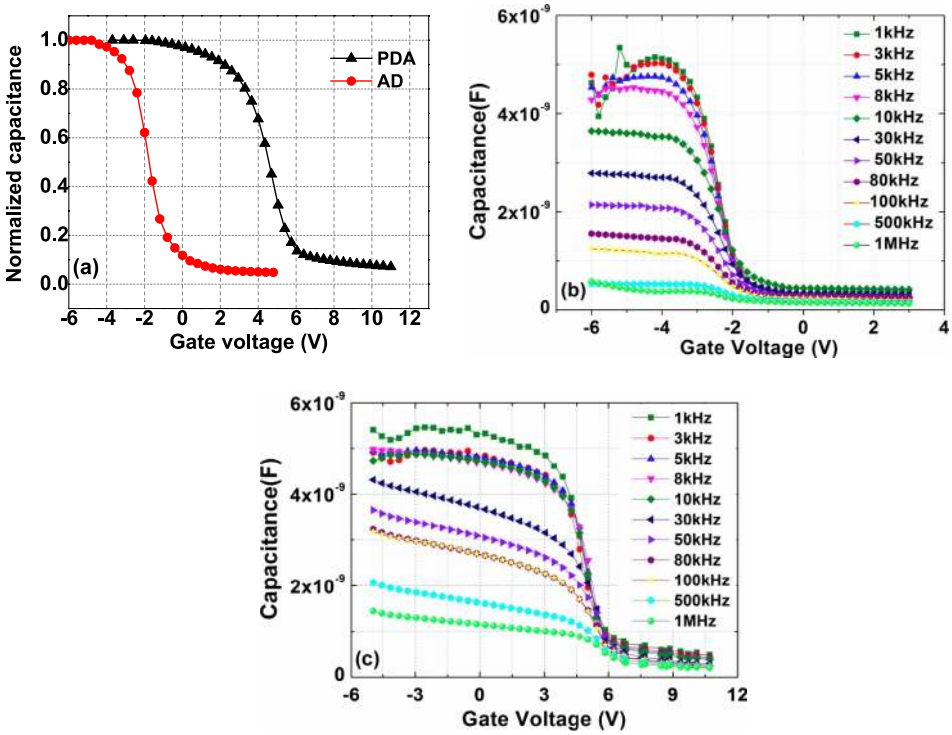

FIG. 1. (a) Normalized capacitance–voltage (C–V) plots at 10 kHz for AD and PDA films, C–V as a function of frequency for (b) AD and (c) PDA films.

properties, all the measured C-V-G curves were first corrected for parasitic free C-V-G curves using "dual-frequency five-element circuit model" proposed in Ref. 20.

The effective fixed charge density (Q_f) for both AD and PDA films was estimated from the flatband voltage (V_{fb}) of the low frequency C-V curve using the following equation:[13]

$$Q_f = \frac{C_{ox}\left(W_{ms} - V_{fb}\right)}{A * q} \tag{1}$$

where $W_{ms} = -0.97$ V is the estimated work function difference between metal (Al) and semiconductor (CIGS) for an acceptor concentration of $N_A = 5 \times 10^{15}$ cm^{-3}, C_{ox} is the oxide capacitance per unit area, q is the elementary electric charge and A is the top Al gate area. The extracted V_{fb} values as a function of temperature for the AD and PDA films are in the range of −2.1 to −2.7 V and +3.3 to +3.6 V, resulting in a fixed oxide charge density of +1.6 to $+2.5 \times 10^{12}$ cm^{-2} and −9.4 to -11.0×10^{12} cm^{-2}, respectively. These results reveal that the field-effect passivation due to negative fixed charges is activated only for post-deposition annealed Al_2O_3 films, and that the extracted negative fixed charge density Q_f is within a range similar to that observed on silicon surfaces.[9–12] This indicates that the field-effect passivation quality achieved by the PDA films on CIGS surfaces is comparable to that achieved by ALD Al_2O_3 films on silicon surfaces.[9–11] Furthermore, due to the presence of highly negative Q_f values in the PDA films, the net concentration of minority carriers (n_s) at the CIGS surface will be reduced, thereby satisfying one of the requirements to reduce the surface recombination rate (U_s) according to the Shockley–Read–Hall formalism.[21,22]

Another possibility for reducing U_S is to reduce the interface trap charge density (D_{it}) at the Al_2O_3/CIGS interface, since it reflects the chemical passivation quality at the interface. Reliable estimations of D_{it} on the AD and PDA films were performed using normal and full conductance methods over limited band energies (i.e., near band edge).[14,23] Figs. 2(a) and 2(b) shows the normalized interface-trap parallel conductance over angular frequency (G_p/ω) as a function of the small-signal ac frequency (f) for the AD and PDA films, respectively. The plots of G_p/ω vs. f were generated for a broad range of temperatures (100-260 K, in steps of 20 K) for depletion

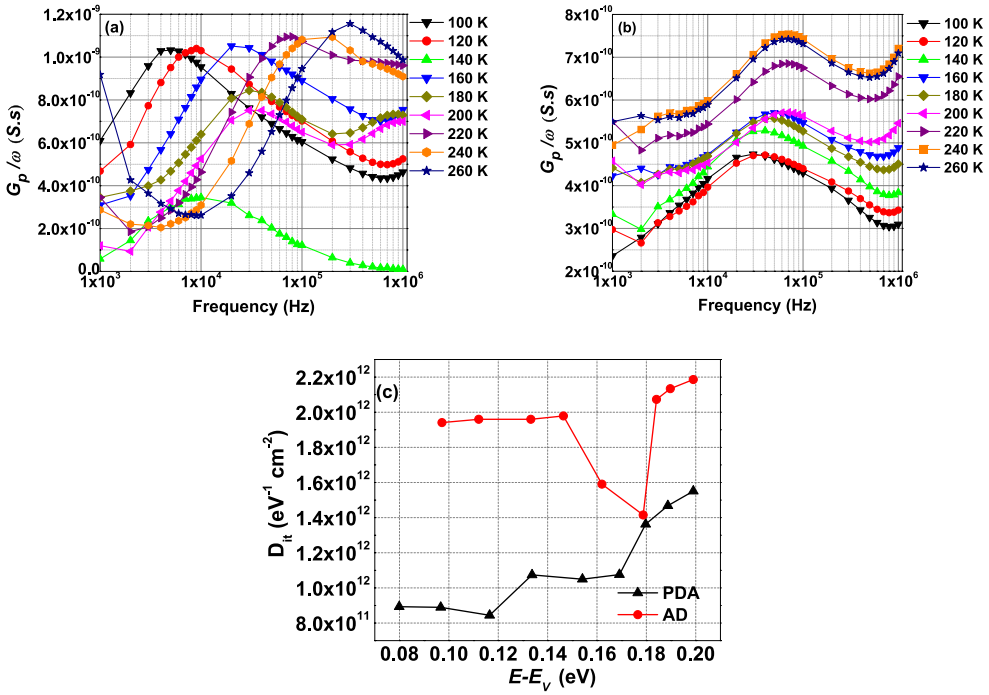

FIG. 2. Measured G_p/ω as a function of applied AC frequency at different temperatures for the (a) AD films, (b) PDA films and (c) extracted interface-trap charge density as a function of the bandgap energy.

gate voltages. The D_{it} values were estimated from the peak maximum of the G_p/ω vs. f plot, which corresponds to the energy loss at the interface as a consequence of trapping and de-trapping mechanisms. The relation between $G_p(\omega)$ and the trap density D_{it} is given as:[14]

$$\frac{G_p(\omega)}{\omega} = \frac{qD_{it}}{2\omega\tau_{it}} \ln[1 + (\omega\tau_{it})^2] \tag{2}$$

from which one can deduce:

$$D_{it} = \frac{2.5}{A * q}\left(\frac{G_p}{\omega}\right)_{max} \tag{3}$$

where $(G_p/\omega)_{max}$ is the maximum $(G_p(\omega)/\omega)$ value and τ_{it} is the interface-trap response time constant. The extracted D_{it} values as a function of temperature for the AD and PDA films are in the range of $(1.4–2.2) \times 10^{12}$ eV^{-1} cm^{-2} and $(8.3–11.0) \times 10^{11}$ eV^{-1} cm^{-2}, respectively, and the corresponding D_{it} as a function of energy bandgap is shown in Fig. 2(c).

Table I represents the range of Q_f and D_{it} values extracted for the AD and PDA films in the depletion to mid-gap voltage regimes at 300 K on several devices (mapping). These results indicate an improved chemical passivation for the PDA samples compared with the AD samples. However, the D_{it} values obtained for the PDA samples are slightly higher than those obtained for the ALD Al_2O_3 films on silicon surfaces.[9–12] One possible reason for such low D_{it} values on silicon surfaces is the growth of a thin (1–2 nm) SiO_x interfacial layer, which improves the chemical

TABLE I. Extracted Q_f and D_{it} at 300K for AD and PDA films. The + and − polarities represent positive and negative fixed charges in the Al_2O_3 film, respectively.

Sample	No. of samples	Q_f (cm^{-2})	D_{it} (eV^{-1} cm^{-2})
AD	10	$+(8.1–33.0)\times10^{11}$	$(1.2–3.4)\times10^{12}$
PDA	10	$-(9.4–20.0)\times10^{12}$	$(8.1–15.0)\times10^{11}$

passivation quality at the Al_2O_3/*c*-Si interface.[9,12] This leaves sufficient room for further research on the interface chemistry of Al_2O_3/CIGS that is beyond the scope of this study.

The passivation quality achieved by the AD and PDA films were further investigated by estimating the minority carrier concentration at the CIGS surface. These estimations were performed using a one-dimensional numerical solar cell capacitance simulator (SCAPS-1D) model of an Al/Al_2O_3/CIGS/Mo structure. In order to maintain the electrical contact in such 1D simulations, the Al_2O_3 films were modeled with characteristics similar to the CIGS thin film; these films differ only with respect to thickness (22.5 nm). The mean values of the experimentally extracted Q_f and D_{it} range shown in Table I were inputted as bulk (i.e. in the 22.5 nm Al_2O_3 layer) and interface (i.e. in-between Al_2O_3/CIGS) charges in the simulator, respectively, where the CIGS baseline parameters for the simulations were obtained from Ref. 24. The corresponding electron (n_s) and hole (p_s) concentrations at the CIGS surface for the AD and PDA samples were simulated under one-sun illumination conditions (100 mW/cm^2, air mass 1.5).

Fig. 3 represents the n_s and p_s concentration profiles estimated using SCAPS simulations for the AD and PDA films as a function of distance from the Al_2O_3/CIGS interface. These estimations were performed using the films' corresponding Q_f and D_{it} values. The results suggest that for the AD films, because of the presence of positive fixed charges (Q_f), an inversion layer of minority charges (i.e., $n_s > p_s$) is formed beneath the Al_2O_3 film. In contrast, in the PDA films, the high density of negative Q_f in the bulk of the Al_2O_3 film drives the CIGS surface into accumulation mode (i.e., $p_s > n_s$). Under such accumulation conditions, the valence and conduction bands bend upwards, resulting in a built-in electric field that hinders the minority carriers (i.e., up hill for electrons) from recombining at the interface.[8] The surface concentration of minority carriers (n_s) for the PDA films is approximately eight orders of magnitude lower than that for the AD films. Indeed this can reduce the surface recombination rate to a great extent, depending on the magnitude and ratio of electron-to-hole capture cross- sections (σ_n/σ_p) at the Al_2O_3/CIGS interface, reaching levels comparable to those obtained on p-type silicon surfaces with ALD Al_2O_3 passivation.[9–12]

The electronic properties of the ALD Al_2O_3/CIGS surfaces and interface have been experimentally extracted for the first time. On the basis of *C*–*V* and *G*-*f* measurements, the PDA films exhibit a high density of negative fixed charges in combination with slightly lower interface trap charges as compared to the AD films. This results in a significant reduction of the surface recombination velocity at the Al_2O_3/CIGS interface. Through experimental extractions and numerical simulations, we confirm that the passivation quality improves considerably from AD to post-annealed films,

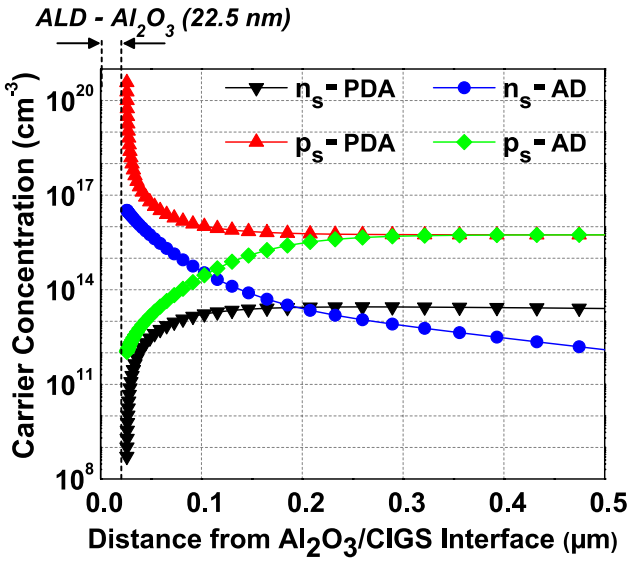

FIG. 3. Numerically simulated surface concentration of electrons and holes for the AD and PDA films for a uniform CIGS acceptor concentration of $N_A = 5 \times 10^{15}$ cm^{-3} under one-sun illumination conditions (100 mW/cm^2, air mass 1.5).

primarily due to the negative fixed charge-induced field-effect passivation over chemical passivation in post-annealed films. This result indicates that the annealing of the ALD Al_2O_3 film plays a vital role in activating the field-effect passivation and in reducing the overall recombination losses at the interface. As a consequence of the excellent passivation quality of the optimized (annealed) ALD Al_2O_3 films, they can be considered as a promising candidate to passivate the CIGS/Mo interface to substantially enhance the cell performance. We expect our work will not only help to understand the passivation mechanism involved at ALD Al_2O_3/CIGS interface, but also to quantify the rear surface passivation quality of the CIGS solar cells i.e. Mo/Al_2O_3/CIGS interfaces in a better way.

This work is supported by FRS-FNRS Belgium, the Swedish Science Foundation (VR), and, the Swedish Energy Agency. B. Vermang acknowledges the financial support of the Flemish Research Foundation FWO (mandate 12O4215N). R. Kotipalli would like to thank the teams of the nanofabrication-shared facility WINFAB and the electrical characterization WELCOME platforms at UCL for their technical support.

[1] P. Jackson, D. Hariskos, R. Wuerz, O. Kiowski, A. Bauer, T. M. Friedlmeier, and M. Powalla, Phys. Status Solidi RRL **9**, 28 (2014).
[2] A. Chirilă, P. Reinhard, F. Pianezzi, P. Bloesch, A. R. Uhl, C. Fella, L. Kranz, D. Keller, C. Gretener, H. Hagendorfer, D. Jaeger, R. Erni, S. Nishiwaki, S. Buecheler, and A. N. Tiwari, Nature Materials **12**, 1107 (2013).
[3] P. Reinhard, B. Bissig, F. Pianezzi, H. Hagendorfer, G. Sozzi, R. Menozzi, C. Gretener, S. Nishiwaki, S. Buecheler, and A.N Tiwari, Nano Lett. **15**, 3334 (2015).
[4] B. Vermang, J. T. Wätjen, V. Fjällström, F. Rostvall, M. Edoff, R. Kotipalli, F. Henry, and D. Flandre, Prog. Photovolt: Res. Appl. **22**, 1023 (2014).
[5] B. Vermang, J. T. Wätjen, C. Frisk, V. Fjällström, F. Rostvall, M. Edoff, P. Salomé, J. Borme, N. Nicoara, and S. Sadewasser, IEEE Journal of Photovoltaics. **4**, 1644 (2014).
[6] R. Kotipalli, B. Vermang, V. Fjällström, M. Edoff, R. Delamare, and D. Flandre, Phys. Status Solidi RRL **9**, 157 (2015).
[7] J. Joel, B. Vermang, J. Larsen, O. Donze-Gargand, and M. Edoff, Phys. Status Solidi RRL, Phys. Status Solidi RRL (2015).
[8] W. W. Hsu, J. Y. Chen, T. H. Cheng, S. C. Lu, W. S. Ho, Y. Y. Chen, Y. J. Chien, and C. W. Liu, Appl. Phys. Lett. **100**, 023508 (2012).
[9] G. Dingemans and W. M. M. Kessels, J. Vac. Sci. Technol. A **30**, 040802 (2012).
[10] B. Hoex, S.B.S. Heil, E. Langereis, M.C.M. van de Sanden, and W.M.M. Kessels, Appl. Phys. Lett. **89**, 042112 (2006).
[11] F. Werner, A. Cosceev, and J. Schmidt, Energy Procedia **27**, 319 (2012).
[12] R. Kotipalli, R. Delamare, O. Poncelet, X. Tang, L. A. Francis, and D. Flandre, EPJ Photovoltaics. **4**, 45107 (2013).
[13] D. K. Schroder, *Semiconductor material and device characterization* (John Wiley & Sons Inc, Hoboken, 2006).
[14] E. H. Nicollian and J. R. Brews, *MOS (Metal Oxide Semiconductor) Physics and Technology* (Wiley, New York, 1982).
[15] Y. Yuan, L. Q. Wang, B. Yu, B. H. Shin, J. Ahn, P. C. McIntyre, P. M. Asbeck, M. J. W. Rodwell, and Y. Taur, IEEE Electron Device Lett. **32**, 485 (2011).
[16] G. W. Paterson, M. C. Holland, I. G. Thayne, and A. R. Long, J. Appl. Phys. **111**, 074109 (2012).
[17] G. Brammertz, A. Alian, D. H. C. Lin, M. Meuris, M. Caymax, and W. E. Wang, IEEE Trans. Electron Devices **58**, 3890 (2011).
[18] E. J. Kim, L. Q. Wang, P. M. Asbeck, K. C. Saraswat, and P. C. McIntyre, Appl. Phys. Lett. **96**, 012906 (2010).
[19] E. H. Nicollian and A. Goetzberger, Bell System Tech. J. **46**, 1055 (1967).
[20] W.H. Wu and B.Y. Tsui, Electron Device Lett. IEEE **27** (2006).
[21] W. Shockley and W. T Read, Physics Review **87**, 835 (1952).
[22] A. G. Aberle, S. Glunz, and W. Warta, J. Appl. Phys. **71**, 4422 (1992).
[23] K. Martens, C. O. Chui, G. Brammertz, B. De Jaeger, D. Kuzum, M. Meuris, M. M. Heyns, T. Krishnamohan, K. Saraswat, H. E. Maes *et al.*, IEEE Trans. Electron Devices **55**, 547 (2008).
[24] M. Gloeckler, Ph.D. thesis, Colorado State University, 2002.